Journal of Magnetic Resonance 233 (2013) 1–6

Contents lists available at SciVerse ScienceDirect

Journal of Magnetic Resonance

journal homepage: www.elsevier.com/locate/jmr

High-resolution optically-detected magnetic resonance imaging in an ambient magnetic field

Songtham Ruangchaithaweesuk, Vasudeva Chintamsetti, Li Yao, Te-Wei Tsai, Shoujun Xu *

Department of Chemistry, University of Houston, Houston, TX 77204, USA

ARTICLE INFO

Article history:
Received 7 March 2013
Revised 23 April 2013
Available online 9 May 2013

Keywords:
Ultralow-field MRI
Zoom-in method
Concomitant field effect
Optical detection
Filling factor
Atomic magnetometry

ABSTRACT

Magnetic resonance imaging (MRI) in an ultralow magnetic field usually has poor spatial resolution compared to its high-field counterpart. The concomitant field effect and low signal level are among the major causes that limit the spatial resolution. Here, we report a novel imaging method, a zoom-in scheme, to achieve a reasonably high spatial resolution of 0.6 mm × 0.6 mm without suffering the concomitant field effect. This method involves multiple steps of spatial encoding with gradually increased spatial resolution but reduced field-of-view. This method takes advantage of the mobility of ultralow-field MRI and the large physical size of the ambient magnetic field. We also demonstrate the use of a unique gradient solenoid to improve the efficiency of optical detection with an atomic magnetometer. The enhanced filling factor improved the signal level and consequently facilitated an improved spatial resolution.

1. Introduction

Ultralow-field MRI is usually performed in a magnetic field equal to or lower than the Earth's magnetic field (~50 μT) [1–5]. One unique advantage and significant application of ultralow-field MRI is the capability to image through metal because of the much greater skin depth of low-frequency radiation. For instance, the skin depth of 2.1-kHz electromagnetic wave, which corresponds to the Larmor frequency of protons at 50 μT, is on the order of 1 cm in typical metals, whereas the skin depth is only a few micrometers for 500-MHz radiation [6]. In addition, magnetically heterogeneous samples can be studied in an ultralow magnetic field because the field distortion induced by the magnetic susceptibility of the sample is proportional to the magnetic field strength. Furthermore, ultralow-field MRI offers the advantages of portability and low cost; these advantages allow it to be employed in remote areas and in developing regions.

Because of the relatively poor sensitivity of the inductive coils in an ultralow magnetic field, an alternative detection technique is usually used. Superconducting quantum interference devices (SQUIDs) have been used for ultralow-field MRI by several research groups [7–11]. Optical detection with atomic magnetometers was later reported for ultralow-field MRI. Initially, imaging of flow was demonstrated with a remote detection scheme [12]. Then, Savukov et al. showed the first ultralow-field MRI of static samples using atomic magnetometers [13]. Recently, optically detected MRI was used to investigate flow in porous metallic materials to show that ultralow-field MRI is a unique technique for revealing defects in porous metals [14]. A third alternative technique, using magneto-resistive sensors, has also been successfully demonstrated for ultralow-field MRI [15].

A major challenge for ultralow-field MRI has been poor spatial resolution regardless of which detection technique is used. In addition to the low nuclear magnetization in an ultralow field even via pre-polarization compared to that in a high magnetic field (>1 T), one main reason for the poor spatial resolution is the concomitant field effect, which imposes an upper limit on the gradient field [16,17]. For instance, for a 10 × 10 imaging of a 1 cm × 1 cm area, the maximum gradient field is approximately 5 μT/cm to avoid substantial image distortion. The situation is particularly severe under ambient conditions because the significant heterogeneity of the magnetic field imposes a lower limit on the gradient field. For example, the homogeneity of the ambient magnetic field in a laboratory environment is approximately 0.1–0.2 μT/cm. This value sets a lower limit of approximately 1 μT/cm for the gradient field. Therefore, the appropriate range for the amplitude of the gradient field is small. Consequently, the spatial resolution is constrained. Several methods for image correction have been proposed and have been experimentally implemented [18–20]. However, the spatial resolution for ultralow-field MRI has not reached sub-millimeter resolution for both of the in-plane axes.

An additional issue that limits the spatial resolution of ultralow-field MRI is the low detection efficiency of the alternative techniques. For optical detection with atomic magnetometers, the atomic sensor is usually placed in the vicinity of the nuclear

* Corresponding author. Fax: +1 713 743 2709.
E-mail address: sxu7@uh.edu (S. Xu).

1090-7807/$ - see front matter © 2013 Elsevier Inc. All rights reserved.
http://dx.doi.org/10.1016/j.jmr.2013.05.001

spins. The filling factor is not as optimal as that of an inductive coil, which usually encloses the entire sample. Although the innovative idea of using a flux transformer has been successfully demonstrated, this method only has good sensitivity at approximately 100 kHz because it is based on Faraday induction [13,21]. Thus, this method is not suitable for investigating metallic materials. New configurations are needed to improve the filling factor in ultralow magnetic fields, and this improvement will eventually also improve the spatial resolution.

Here, we report a zoom-in imaging method that overcomes the concomitant field effect in an ambient magnetic field. Sub-millimeter resolution has been obtained through the clear revelation of a 0.6 mm gap between two flow channels. Detection is achieved with an optical magnetometer. Through the implementation of a gradient solenoid, the filling factor, and hence, the detection efficiency, is significantly improved. The resultant higher signal level enhanced the spatial resolution.

2. Experimental methods

Fig. 1a shows the concept of the zoom-in method. Assuming a field of view (FOV) of 10 cm × 10 cm, a 100 × 100 grid is needed to achieve spatial resolution of 1 mm × 1 mm (Fig. 1a, left). Such a large number of encoding steps will most likely make the maximum gradient field comparable to or larger than the ambient field, giving that the gradient field has a lower limit determined by the field inhomogeneity. Therefore, the concomitant field effect will be severe. In other words, it is difficult to obtain 1 mm × 1 mm resolution. However, we can instead focus on one (or a few) region(s) of interest by initially imaging a 10 × 10 grid. The significantly reduced number of steps will not cause the concomitant field effect. Then, the center of the gradient stack is moved to the region of interest. A second 10 × 10 image on the reduced field of view is performed (Fig. 1a, right). The net result is that for the region of interest, a high resolution of 1 mm × 1 mm is obtained and the concomitant field effect is avoided because of the reduced field of view.

The zoom-in method requires two conditions. One condition is that the gradient stack be mobile. This condition is easily satisfied for ultralow-field MRI because the gradient coils are open, lightweight, and use very low current; thus, the coils have high mobility. Fig. 1b shows the gradient stack mounted on a two-dimensional translation stage. The other requirement is that the magnetic field B_0 be large in size, so that there is room to move the gradient coils to obtain different FOVs and so that the movement is not physically restricted by the magnet. This requirement is easily met by the ambient magnetic field produced by the Earth.

An optical atomic magnetometer is used to detect nuclear magnetization with a remote detection scheme (Fig. 1c). Here, prepolarization is achieved with a 2-T permanent magnet. Spatial encoding is performed in the ambient magnetic field. The encoded nuclear spins in water flow inside the detection region, which is inside a multilayer magnetic shield where an atomic sensor resides. The sensitivity of the atomic magnetometer is approximately 80 fT/(Hz)$^{1/2}$ for near-dc magnetic signals.

The imaging phantom is shown in Fig. 2a. The phantom consists of two channels, both 4.0 mm in height but with different widths; one channel is 1.9 mm wide, and the other is 1.6 mm. The gap between the channels is 0.6 mm. The overall length of the phantom is 10 mm. The translation stages, one for the x-axis and one for the z-axis, have a movement range of 25 mm.

The pulse sequence is similar to the phase encoding sequence used previously (Fig. 2b) [12,14]. The excitation frequency is 2.045 kHz, which corresponds to a magnetic field strength of 48 μT. The duration of the 90° pulse is 6 ms, and the gradient field duration is 5 ms. Phase cycling is used for the second 90° pulse. The field inhomogeneity is measured to be 0.1 μT/cm perpendicular to B_0 (x- and y-axes) and 0.2 μT/cm along B_0 (z-axis). The gradient strength $\Delta G_{x,y}$ was 3.5 μT/cm for the first step of the zoom-in process. For the second encoding step, after moving the gradient stack, ΔG_x was 7.0 μT/cm. ΔG_y was 3.5 μT/cm.

A gradient solenoid was used to guide the nuclear spins while the spins flowed into the detection region inside the magnetic shield (Fig. 3). The winding was tight at the left side, which was

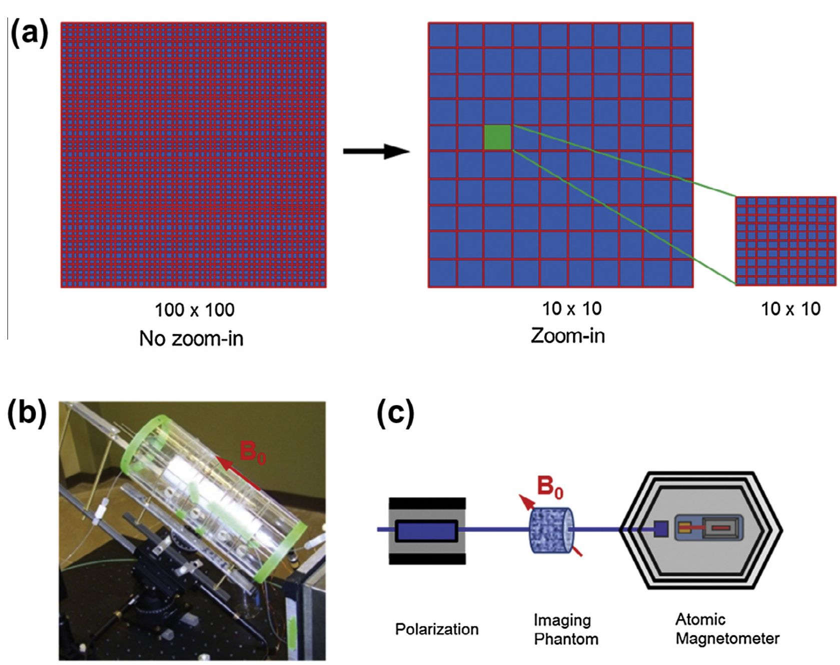

Fig. 1. Experimental details: (a) schematic of the zoom-in method. The left panel shows the ordinary imaging method with no zoom-in. The right panel shows the zoom-in method, which consists of two 10 × 10 grids that achieve the same spatial resolution as the ordinary 100 × 100 grid, but only for a region of interest (in green); (b) the coil stack is mounted on a two-dimensional translation stage; the orientation of the coil stack is aligned with the ambient magnetic field B_0; (c) scheme showing the optically detected ultralow-field MRI of the flow. (For interpretation of the references to color in this figure legend, the reader is referred to the web version of this article.)